Physics Letters B 797 (2019) 134899

Contents lists available at ScienceDirect

Physics Letters B

www.elsevier.com/locate/physletb

Effects of a non-zero strangeness-chemical potential in strong interaction models

Ayon Mukherjee [a,b,*], Abhijit Bhattacharyya [c], Stefan Schramm [a,b]

[a] Frankfurt Institute for Advanced Studies, Ruth-Moufang-Straße 1, D-60438 Frankfurt am Main, Germany
[b] Institut für Theoretische Physik, Goethe Universität Frankfurt, Max-von-Laue-Straße 1, D-60438 Frankfurt am Main, Germany
[c] Department of Physics, University of Calcutta, 92, Acharya Prafulla Chandra Road, Kolkata 700009, India

ARTICLE INFO

Article history:
Received 6 August 2018
Received in revised form 20 March 2019
Accepted 17 June 2019
Available online 30 August 2019
Editor: W. Haxton

Keywords:
Strangeness
QCD phase diagram
Effective QCD model

ABSTRACT

The effect of a non-zero strangeness chemical potential on the strong interaction phase diagram has been studied within the framework of the SU(3) quark-hadron chiral parity-doublet model. Both, the nuclear liquid-gas and the chiral/deconfinement phase transitions are modified. The first-order line in the chiral phase transition is observed to vanish completely, with the entire phase boundary becoming a crossover. These changes in the nature of the phase transitions are expected to modify various susceptibilities, the effects of which might be detectable in particle-number distributions resulting from moderate-temperature and high-density heavy-ion collision experiments.

One of the primary foci of the ongoing, and upcoming, ultra-relativistic heavy-ion collision (HIC) experiments at RHIC in Brookhaven, at the LHC at CERN or at the future facilities, like FAIR at GSI and NICA in Dubna, is to probe the nature of strongly interacting matter under extreme conditions of temperatures and densities. However, even for these conditions strong interactions are not in the perturbative regime and are therefore extremely difficult to solve directly from first principles.

While Lattice QCD (LQCD) provides the most direct approach for studying high-temperature systems [1,2], it is plagued by the familiar fermion sign-problem [3–9] at non-vanishing baryo-chemical potentials. Effective Lagrangian models [10–31], on the other hand, provide a much more tractable alternative to the study of non-perturbative, strongly-interacting matter. Following this approach, in Ref. [32], within an extended hadron-quark parity-doublet model, the QCD phase diagram and thermal fluctuations in an HIC have been studied, using the cumulants of conserved charges for a range of temperatures (T) and baryo-chemical potentials (μ_B), at zero strangeness- (μ_S) and isospin-chemical potentials (μ_I).

However, the effects of a non-zero μ_S on the QCD phase-diagram and the fluctuations for low densities have been investigated in recent LQCD calculations and Hadron Resonance Gas (HRG) model (comparative) studies [33–44]. On the other hand, the influence of a non-zero μ_I on the chiral phase transition can, in principle, be experimentally tested to some degree by varying projectile and target nuclei. It has been studied theoretically, using both effective-model and LQCD approaches [45–50].

From fitting observed particle ratios, μ_S has been deduced to have a value of ∼2%–30% of μ_B, while μ_I remains small, at around 2%–5% of μ_B [10,51–53]. These values illustrate that the strangeness- and isospin-chemical potentials, though small, are not entirely negligible. It is therefore worthwhile to study the QCD phase-diagram with non-zero isospin-, strangeness- and baryo-chemical potentials. This includes potential fluctuations in the fire-ball creating areas with positive and negative net-strangeness and net-isospin, respectively.

Motivated by these considerations, in this paper the authors focus on the strangeness aspect of a system at high-to-moderate temperatures and high densities. The model being used to study the effects of a non-zero μ_S (with μ_I = 0) is the Quark-Hadron Chiral Parity Doublet Model (QχP), which is a low-energy, effective SU(3) chiral model, which has been previously used in Refs. [32,54]. After a brief description of the model and the slight modifications done to its parametrization, the results are presented and discussed, and conclusions are given. For a more detailed explanation of the model itself, see Refs. [55–58].

In parity-doublet formulations the Lagrangian can contain an explicit mass term for the baryons that does not break chiral symmetry [59]. The signature for chiral symmetry restoration is the

* Corresponding author.
E-mail address: mukherjee@fias.uni-frankfurt.de (A. Mukherjee).

https://doi.org/10.1016/j.physletb.2019.134899

degeneracy of the usual baryons and their respective negative-parity partner states, which are grouped in doublets $N = (N^+, N^-)$ as discussed in Refs. [59,60]. Taking into account the scalar and vector condensates in mean-field approximation, the resulting Lagrangian $\mathcal{L}_B$ reads as [58]:

$$\mathcal{L}_B = \sum_i (\bar{B}_i i\partial\!\!\!/ B_i) + \sum_i \left(\bar{B}_i m_i^* B_i\right) + \sum_i \left(\bar{B}_i \gamma_\mu (g_{\omega i}\omega^\mu + g_{\rho i}\rho^\mu + g_{\phi i}\phi^\mu) B_i\right) , \quad (1)$$

summing over the states of the baryon octet. The effective masses of the baryons (assuming the matter to be isospin-symmetric) are:

$$m_{i\pm}^* = \sqrt{\left[(g_{\sigma i}^{(1)}\sigma + g_{\zeta i}^{(1)}\zeta)^2 + (m_0 + n_s m_s)^2\right]} \pm g_{\sigma i}^{(2)}\sigma \pm g_{\zeta i}^{(2)}\zeta , \quad (2)$$

with $g_i^{(j)}$'s as the coupling constants of the baryons with the scalar fields σ $(\langle\overline{\psi}\psi\rangle)$ and ζ $(\langle\overline{s}s\rangle)$. In addition, there is an SU(3) symmetry-breaking mass term proportional to the strangeness, n_s, of the respective baryon. Note that in the parity doublet model, there are two linear couplings of the scalar fields $g_\sigma^{(1)}, g_\zeta^{(1)}$ to the baryonic fields, where the second one generates the mass splitting of the parity doublet states. In order to avoid introducing too many parameters, we assume that the splitting of the various baryon species and their respective parity partners has the same value for all baryons. The hyperonic vector interactions are tuned to generate phenomenologically acceptable optical potentials of the hyperons in ground-state nuclear matter. The relevant parameters have been tabulated in Ref. [32]. For the calculations done in this paper, the parametrization is kept similar to that used earlier, the only difference being the omission of the baryon decuplet, and other higher resonances, from the particle mixture, which simplifies the discussion without major quantitative changes.

In many-body systems, like those resulting from HICs, a chemical potential can be associated with each of the conserved charges of the system. In an HIC's case, the corresponding charges are the baryon-number, isospin and strangeness [61–63], because of the short time elapsed between the formation of the fireball and the chemical, and kinetic, freeze-outs, assuming strangeness equilibration. During this time, only strong interactions play an important role, while electroweak interactions are practically negligible. As first argued in Ref. [64], strangeness might be abundantly produced in the deconfined phase through gluon-gluon fusion, during the early stages of the system's evolution. The strange quarks are later rapidly redistributed in the hadronic phase, via multi-mesonic interactions, when the system is close to the transition [65].

Although the total strangeness of the entire system (fireball) remains zero throughout its formation and evolution, local distributions of non-zero strangeness (and anti-strangeness) regions could be formed as a result of fluctuations, resulting in a non-uniform distribution of strangeness within the system [66–69]. These local sub-systems can be considered as being in thermal equilibrium with the rest of the system; since they are considerably smaller in size compared to the entire system. Thus, they can be adequately described by a grand-canonical ensemble.

The pressure (P) for such a thermalised system can be written as:

$$P = -E + TH + \sum_j \left(B_j\mu_{B_j} + S_j\mu_{S_j} + I_j\mu_{I_j}\right) , \quad (3)$$

with E, T, H, μ, B_j, S_j and I_j representing the energy, temperature, entropy, chemical potential, baryon-number, strangeness and isospin, respectively, of the different particle species; and the relative sign between B and S being always negative. In the quark phase, strange-quarks (or anti-quarks) carry a baryon number of 1/3 (or −1/3).

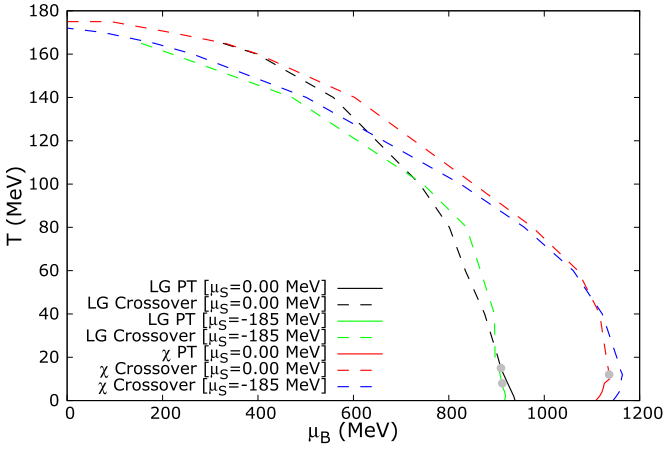

Fig. 1. $T - \mu_B$ phase-diagram, showing the LG and chiral transitions at $\mu_S = 0$ and −185 MeV.

For the purpose of this paper isospin effects are not considered and Eqn. (3) reduces to:

$$P = -E + TH + \sum_j \left(B_j\mu_{B_j} + S_j\mu_{S_j}\right) . \quad (4)$$

Due to a non-zero μ_S, depending on the sign, hyperon thresholds are lowered to values below, or close to, the masses of the non-strange baryons. Thus, the hyperonic particles appear in the system at smaller values of μ_B, as compared to the case of $\mu_S = 0$. The hyperons produced have two non-zero quantum numbers (B_j and S_j) and chemical potentials (μ_{B_j} and μ_{S_j}). These changes naturally drive the first-order, nuclear Liquid-Gas (LG) transition to lower values of μ_B, as shown in Fig. 1. At $\mu_S = -185$ MeV, not only is the LG transition line shifted to the left, but also its critical end-point ($T_{\rm CEP}$, $\mu_{B_{\rm CEP}}$) is lowered along the T-axis; from 15 MeV (for $\mu_S = 0$ MeV) to 8 MeV (for $\mu_S = -185$ MeV), weakening the phase boundary to a crossover, earlier than that with a vanishing μ_S. It is also evident from the figure that the chiral first-order transition weakens with larger negative values of μ_S and disappears completely below $\mu_S = -185$ MeV, giving way to a smooth crossover transition, for the full range of temperatures.

In Fig. 2 the normalised scalar field (σ/σ_0) is plotted as a function of μ_B at $T = 0$ MeV. One can observe that the chiral first-order transition actually vanishes at $\mu_S = -175$ MeV. As can be seen in Figs. 3, 4, 5 and 6, the chiral condensate is intimately related to the net-baryon density, and hence, the change in either variable can be used to define the transition [32,70–72]. From the figures, one arrives at the immediate conclusion that, with increasing $|\mu_S|$, these quantities exhibit progressively shallower jumps near the transition, pointing to a weakening of the first-order phase transition. The increase of higher-mass hyperons in the hadronic phase reduces the relative abundance of the lower-mass, non-strange baryons (Figs. 3 and 4). Fig. 5 shows that the strange-quark degrees-of-freedom, already present in the system before the transition (in the hadronic phase), increase, with an increase in $|\mu_S|$; causing the relative contribution of the lighter, non-strange quark degrees-of-freedom to decrease (Fig. 6). By significant couplings to the much stiffer strange-quark condensate ζ, the hyperons gradually push the chiral transition to higher values of μ_B. Since the transition is signalled by an abrupt decrease in σ, to which the nucleons couple more strongly, a lower concentration

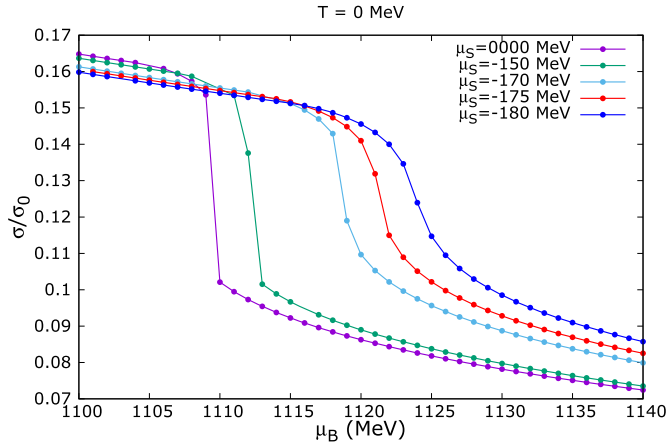

Fig. 2. Normalised chiral condensate, as a function of μ_B, for different values of μ_S, at $T = 0$.

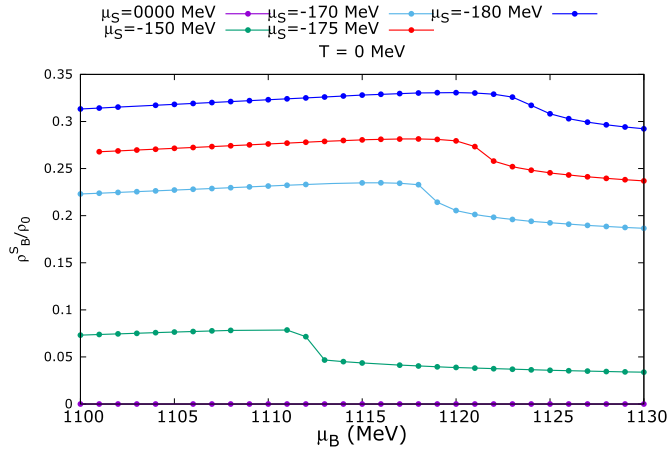

Fig. 3. Relative abundance of hyperons, as a function of μ_B, for different values of μ_S, at $T = 0$.

of these non-strange baryons at moderate μ_B causes the hadronic phase to survive much longer than that for a vanishing μ_S. Moreover, this suppression of the non-strange baryons causes a smoothing of the transition, even at lower values of $|\mu_S|$, as seen in Fig. 2. When the concentration of strange-quarks in the hadronic phase increases further, with higher values of $|\mu_S|$ (Fig. 5), the degrees-of-freedom do not change as drastically across the chiral transition, resulting in a smooth crossover, instead of a sharp first-order, for all strangeness-chemical potentials ≤ -175 MeV and temperatures $\gtrsim$0 MeV.

In Figs. 7 and 8, the strangeness fraction (f_S); defined as:

$$f_S = \frac{\rho_B^S}{\rho_B}\,; \tag{5}$$

is plotted against μ_B, at different temperatures, for $\mu_S = -185$ MeV and 0 MeV, respectively. The baryon number density ρ_B^S includes contributions from both quarks and baryons. In Figs. 9 and 10, the relative abundances of the strange-quarks and hyperons are plotted, while in Figs. 11 and 12, the normalised particle-number-densities; for all quarks and baryons, at different temperatures; are plotted against μ_B, for constant values of μ_S (-185 MeV and 0 MeV, respectively). The normalisation is done using the nuclear saturation density $\rho_0 = 0.15$ fm^{-3}.

As is amply evident from Fig. 8, for $\mu_S = 0$, the system lacks the rich structure, at lower temperatures, visible in Fig. 7. Moreover,

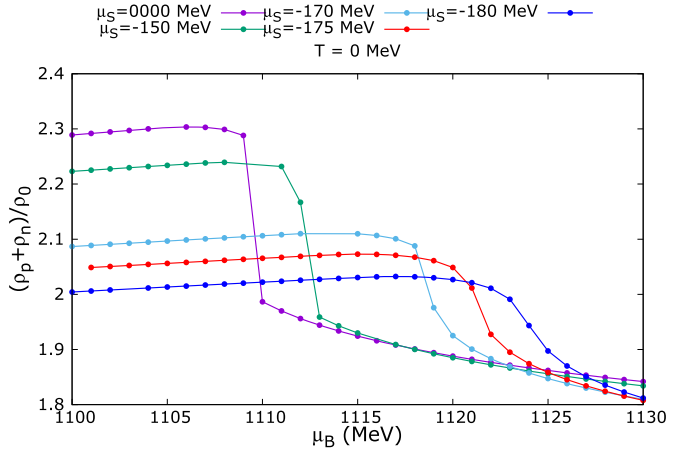

Fig. 4. Relative abundance of non-strange baryons, as a function of μ_B, for different values of μ_S, at $T = 0$.

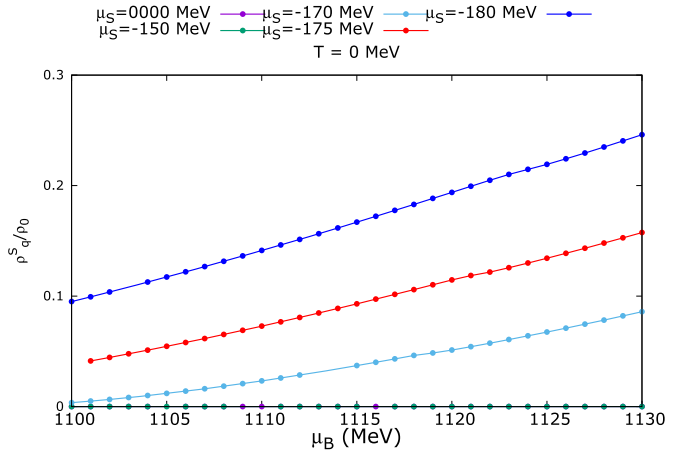

Fig. 5. Relative abundance of strange-quarks, as a function of μ_B, for different values of μ_S, at $T = 0$.

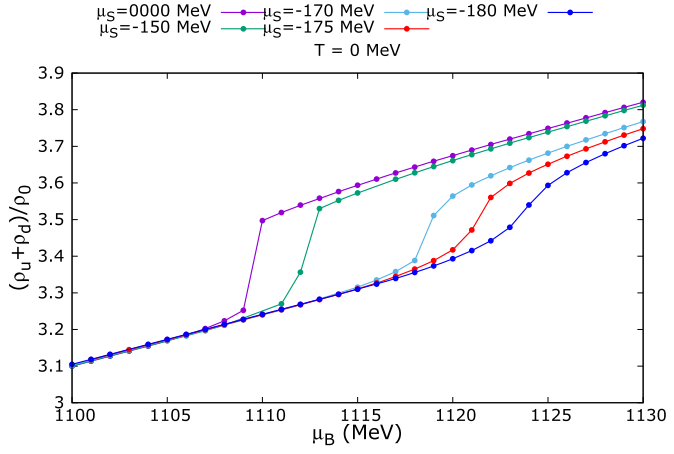

Fig. 6. Relative abundance of non-strange quarks, as a function of μ_B, for different values of μ_S, at $T = 0$.

the curve for $T = 0$ MeV in this figure is buried beneath the $T = 20$ MeV curve. So there is no evidence of any structure between the temperatures 0 and 20 MeV; as corroborated by Fig. 10.

In Fig. 7, the $T = 0$ MeV curve begins exactly after the first-order LG transition, at $\mu_B \sim 920$ MeV. This sudden appearance of

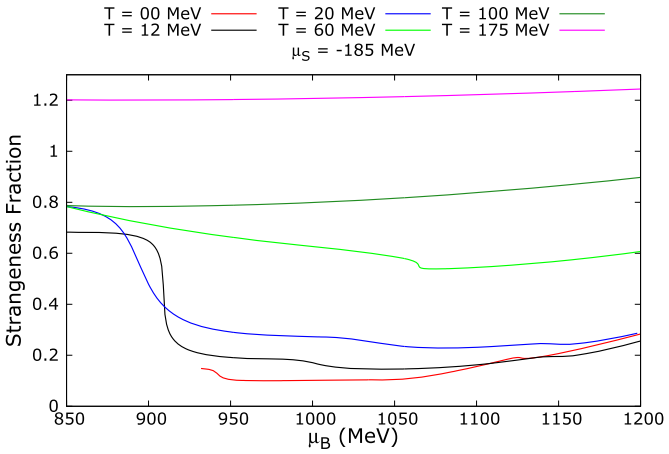

Fig. 7. Strangeness fraction, as a function of μ_B, for different values of T, at $\mu_S = -185$ MeV.

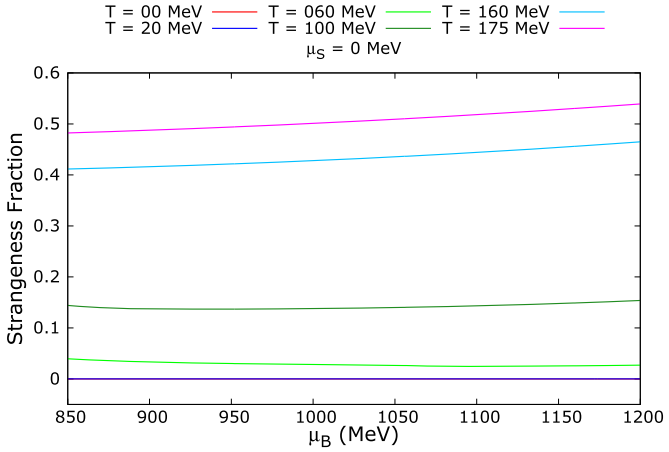

Fig. 8. Same as Fig. 7, at $\mu_S = 0$ MeV.

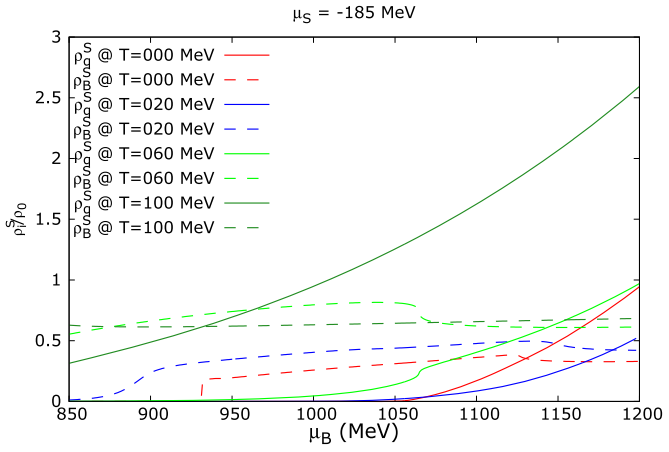

Fig. 9. Relative abundances of strange-quarks and hyperons, as functions of μ_B, for different values of T, at $\mu_S = -185$ MeV.

strangeness can be attributed to the introduction of the Λ and Ξ hyperons to the system – along with other baryons – as can be seen in Fig. 9, thereby making both ρ_B^S and ρ_B non-zero. The shoulder-like dip at $\mu_B \sim 940$ MeV is the result of the early onset of the up- and down-quarks, as seen in Fig. 11.

For the $T = 12$ and 20 MeV curves in Fig. 7, f_S decreases drastically after the LG transition. This is because, right after the

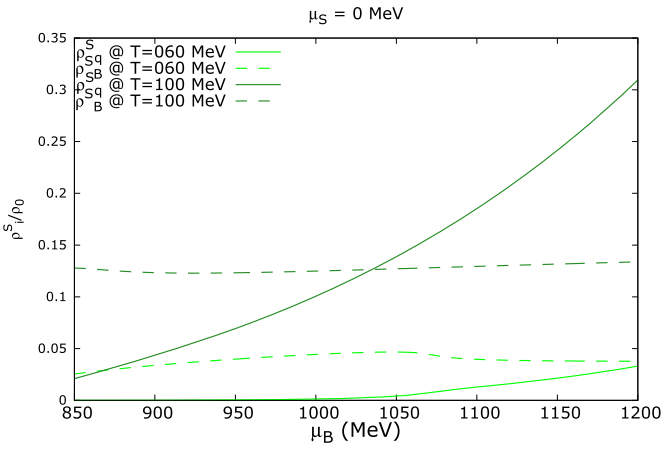

Fig. 10. Same as Fig. 9, at $\mu_S = 0$ MeV. The curves corresponding to temperatures less than 60 MeV are negligibly close to zero and have not been shown.

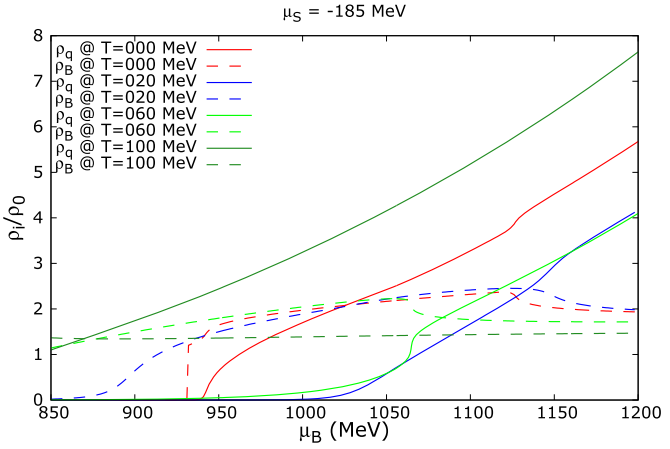

Fig. 11. Relative abundances of quarks and baryons, as functions of μ_B, for different values of T, at $\mu_S = -185$ MeV.

transition, there is a sudden rise in ρ_B, while the strange-particle contribution ρ_B^S does not rise as much, due to the higher masses of the hyperons, which change relatively less strongly across the transition. This drives down the fraction of strangeness in the system, which is slowly revived as the hyperons start increasing in abundance with increasing μ_B, as is evident from the gradual rise of ρ_B^S, for $T = 12$ and 20 MeV, in Fig. 9. With the appearance of the up- and down-quarks (Fig. 11), at around $\mu_B \sim 1000$ MeV, f_S again experiences a slight dip in value. The third and final dips, observed at $\mu_B \sim 1140$ MeV, are caused by the chiral crossover transition (Fig. 1), which is not as sharp compared to the nuclear LG transition. As seen in Figs. 9 and 11, the quarks start dominating the composition of the system, as μ_B increases, from this point onward.

The kink in the $T = 60$ MeV curve (Fig. 7) is caused by the chiral crossover transition, as evident from Figs. 1, 9 and 11. Expectedly, after the transition into the quark sector, the relative abundance of baryons decreases w.r.t. quarks; only in this case, the decrement is much smoother, and smaller, as compared to a first-order transition. The pronounced change in the relative abundance of the quarks observed in Fig. 11, at this temperature is due the interplay between the two different chemical potentials, μ_S and μ_B, and the temperature.

For $T = 100$ and 175 MeV, the respective chiral crossover transitions occur at $\mu_B \sim 840$ and 0 MeV (cf. Fig. 1). As expected, the corresponding f_S curves in Fig. 7 are monotonously increasing

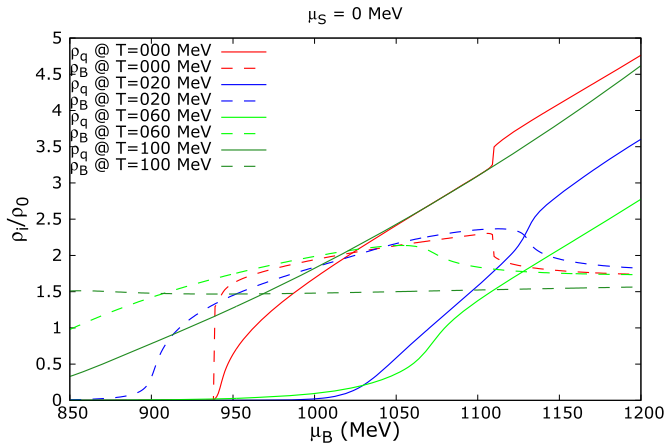

Fig. 12. Same as Fig. 9, at $\mu_S = 0$ MeV.

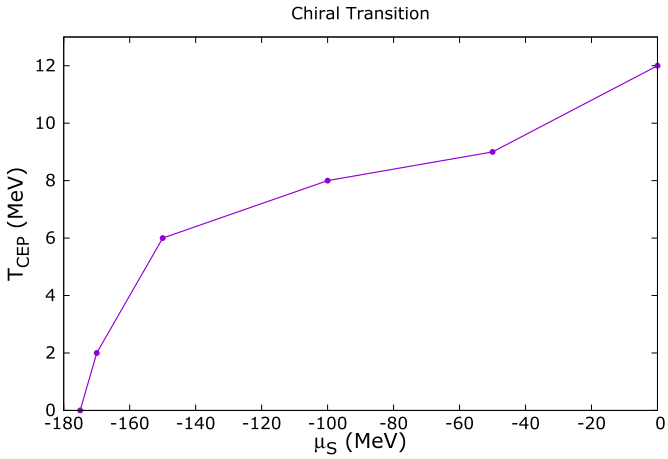

Fig. 13. Critical end-point temperature, for the chiral transition, as a function of μ_S.

functions of μ_B, for the range of values (850–1200 MeV) considered.

The figures, in addition to showing the disappearance of the chiral first-order transition at higher μ_S values, showcase the effect that μ_S has on the system as a whole. The fraction of strangeness in the system, driven by the growing relative abundance of the hyperons and strange-quarks, increases rapidly with μ_B in Figs. 7, 9 and 11. They also grow to much higher values, as compared to what they attained with a zero strangeness-chemical potential, for similar values of μ_B (Figs. 10 and 12). A non-zero μ_S also results in an early onset of the aforementioned strange-particles, as evidenced by the shifting of the kink; corresponding to the chiral transition; in Fig. 7, to progressively lower values of μ_B, with an increase in temperature.

In the case of $\mu_S = 0$ MeV, the strangeness-fraction is observed to be either monotonously increasing, or remaining fairly constant, with μ_B; for all temperatures in Fig. 8. This is to be expected, however, since from Figs. 10 and 12, it is clear that the transitions are primarily driven by the changes in the relative abundances of the non-strange quarks and baryons. But, even in this case, with an increase in temperature, strange-particles with baryon numbers do start to come in due to strange-mesons, in particular kaons. This explains the existence of a non-zero f_S, which increases with an increase in temperature of the system, for a zero strangeness-chemical potential. The slight dip in f_S, at $T = 60$ MeV, is again caused by a sudden increase in ρ_B across the chiral transition (Fig. 1), with ρ_B^S not being able to change as rapidly.

In Fig. 13, the critical end-point temperature is plotted as a function of μ_S. As expected, a considerable, gradual decrease in T_{CEP} is observed, with an increase in the magnitude of μ_S. This re-emphasises the fact that the strangeness-chemical potential directly affects the LG and chiral transitions. The hadronic phase is dominated by hyperons, as μ_S increases in magnitude, suppressing other baryons and resulting in an early onset of both light (u- and d-) and strange quarks; which go on to become a quark state at hight densities.

In conclusion, in this model investigation of quark-hadron systems, one could see that the QCD phase diagram can be significantly affected by a non-zero strangeness-chemical potential, changing the chiral transition from a first-order to a smooth crossover. The critical endpoint in this model appears at low temperatures, which makes such an effect difficult to be directly observed in heavy-ion collisions, but it could have an impact in the higher-temperature smooth transition region as well. Another strangeness-enriched situation is the beta-equilibrated matter in a neutron star, which was investigated in Ref. [54].

A related study could include explicit isospin effects on the behaviour of high-density and high-temperature QCD systems and the role that isospin plays in the system evolution. The fact that non-uniform distributions of isospin in the system are usually very small, is partly compensated by the possibility of experimentally measurable observables. These non-zero isospin-chemical potential effects, and their consequences as experienced by the QχP model, will be investigated in upcoming projects.

The authors would like to thank the Board of Research in Nuclear Sciences (BRNS), India; the Helmholtz International Centre (HIC) for FAIR, the Bundesministerium für Bildung und Forschung (BMBF, Projectnummer: 05P2015), Germany and the Linkage programme of the Alexander von Humboldt foundation, Germany; for their support. They would also like to express their gratitude towards Dr. J. Steinheimer, for his help with the discussions. The calculations for this paper were carried out at the Center for Scientific Computing (CSC) in Frankfurt, Germany.

References

[1] R.A. Soltz, C. DeTar, F. Karsch, S. Mukherjee, P. Vranas, Lattice QCD thermodynamics with physical quark masses, Annu. Rev. Nucl. Part. Sci. 65 (2015) 379–402, https://doi.org/10.1146/annurev-nucl-102014-022157, arXiv:1502.02296.

[2] S. Borsanyi, Z. Fodor, C. Hoelbling, S.D. Katz, S. Krieg, K.K. Szabo, Full result for the QCD equation of state with 2+1 flavors, Phys. Lett. B 730 (2014) 99–104, https://doi.org/10.1016/j.physletb.2014.01.007, arXiv:1309.5258.

[3] G. Aarts, L. Bongiovanni, E. Seiler, D. Sexty, Some remarks on Lefschetz thimbles and complex Langevin dynamics, J. High Energy Phys. 10 (2014) 159, https://doi.org/10.1007/JHEP10(2014)159, arXiv:1407.2090.

[4] G. Aarts, E. Seiler, D. Sexty, I.-O. Stamatescu, On complex Langevin dynamics and zeroes of the measure II: fermionic determinant, PoS LATTICE2016 (2016) 092, arXiv:1611.02931.

[5] G. Aarts, E. Seiler, D. Sexty, I.-O. Stamatescu, Complex Langevin dynamics and zeroes of the fermion determinant, J. High Energy Phys. 05 (2017) 044, https://doi.org/10.1007/JHEP05(2017)044, Erratum: J. High Energy Phys. 01 (2018) 128, https://doi.org/10.1007/JHEP01(2018)128, arXiv:1701.02322.

[6] A. Alexandru, G. Basar, P.F. Bedaque, G.W. Ridgway, N.C. Warrington, Sign problem and Monte Carlo calculations beyond Lefschetz thimbles, J. High Energy Phys. 05 (2016) 053, https://doi.org/10.1007/JHEP05(2016)053, arXiv:1512.08764.

[7] A. Alexandru, G. Bergner, D. Schaich, U. Wenger, Solution of the sign problem in the Potts model at fixed fermion number, arXiv:1712.07585.

[8] K.N. Anagnostopoulos, T. Azuma, J. Nishimura, A practical solution to the sign problem in a matrix model for dynamical compactification, J. High Energy Phys. 10 (2011) 126, https://doi.org/10.1007/JHEP10(2011)126, arXiv:1108.1534.

[9] K.N. Anagnostopoulos, T. Azuma, Y. Ito, J. Nishimura, S.K. Papadoudis, Complex Langevin analysis of the spontaneous symmetry breaking in dimensionally reduced super Yang-Mills models, J. High Energy Phys. 02 (2018) 151, https://doi.org/10.1007/JHEP02(2018)151, arXiv:1712.07562.

[10] P. Braun-Munzinger, K. Redlich, J. Stachel, Particle Production in Heavy Ion Collisions, World Scientific, 2011, pp. 491–599, URL, https://www.worldscientific.com/doi/abs/10.1142/9789812795533_0008.

[11] C. Ratti, M.A. Thaler, W. Weise, Phases of QCD: lattice thermodynamics and a field theoretical model, Phys. Rev. D 73 (2006) 014019, https://doi.org/10.1103/PhysRevD.73.014019, arXiv:hep-ph/0506234.

[12] P.N. Meisinger, M.C. Ogilvie, Chiral symmetry restoration and Z(N) symmetry, Phys. Lett. B 379 (1996) 163–168, https://doi.org/10.1016/0370-2693(96)00447-9, arXiv:hep-lat/9512011.

[13] R. Casalbuoni, D. Dominici, R. Gatto, Effective Lagrangian description of the possible strong sector of the standard model, Phys. Lett. B 147 (6) (1984) 419–424.

[14] C. Csaki, J. Erlich, J. Terning, Effective Lagrangian in the Randall-Sundrum model and electroweak physics, Phys. Rev. D 66 (6) (2002) 064021.

[15] A. Dhar, S.R. Wadia, Nambu—Jona-Lasinio model: an effective Lagrangian for quantum chromodynamics at intermediate length scales, Phys. Rev. Lett. 52 (12) (1984) 959.

[16] T. Hatsuda, T. Kunihiro, Qcd phenomenology based on a chiral effective Lagrangian, Phys. Rep. 247 (5–6) (1994) 221–367.

[17] B.-C. Liu, J.-J. Xie, The k-p$\rightarrow \eta \lambda$ reaction in an effective Lagrangian model, Phys. Rev. C 85 (3) (2012) 038201.

[18] A. Manohar, H. Georgi, Chiral quarks and the non-relativistic quark model, Nucl. Phys. B 234 (1) (1984) 189–212.

[19] C. Rosenzweig, J. Schechter, C. Trahern, Is the effective Lagrangian for quantum chromodynamics a σ model? in: The Large N Expansion in Quantum Field Theory and Statistical Physics: From Spin Systems to 2-Dimensional Gravity, World Scientific, 1993, pp. 351–355.

[20] J. Schechter, Effective Lagrangian with two color-singlet gluon fields, Phys. Rev. D 21 (12) (1980) 3393.

[21] T. Sil, S. Patra, B. Sharma, M. Centelles, X. Vinas, Superheavy nuclei in a relativistic effective Lagrangian model, Phys. Rev. C 69 (4) (2004) 044315.

[22] G. Veneziano, S. Yankielowicz, An effective Lagrangian for the pure $n = 1$ supersymmetric Yang-Mills theory, Phys. Lett. B 113 (3) (1982) 231–236.

[23] M. Abu-Shady, Extended chiral quark models in the framework of quantum chromodynamic: theory and their applications in hot and dense mediums, arXiv:1707.08045.

[24] M.G. Alford, K. Pangeni, A. Windisch, Color superconductivity and charge neutrality in Yukawa theory, Phys. Rev. Lett. 120 (8) (2018) 082701, https://doi.org/10.1103/PhysRevLett.120.082701, arXiv:1712.02407.

[25] A. Banerjee, G. Bhattacharyya, N. Kumar, T.S. Ray, Constraining composite Higgs models using LHC data, J. High Energy Phys. 03 (2018) 062, https://doi.org/10.1007/JHEP03(2018)062, arXiv:1712.07494.

[26] A.N. Atmaja, I. Prasetyo, BPS equations of monopole and Dyon in $SU(2)$ Yang-Mills-Higgs model, Nakamula-Shiraishi models, and their generalized versions from the BPS Lagrangian method, arXiv:1803.06122.

[27] I. Mishustin, J. Bondorf, M. Rho, Chiral symmetry, scale invariance and properties of nuclear matter, Nucl. Phys. A 555 (1993) 215–224, https://doi.org/10.1016/0375-9474(93)90319-S.

[28] E.K. Heide, S. Rudaz, P.J. Ellis, An effective Lagrangian with broken scale and chiral symmetry applied to nuclear matter and finite nuclei, Nucl. Phys. A 571 (1994) 713–732, https://doi.org/10.1016/0375-9474(94)90717-X, arXiv:nucl-th/9308002.

[29] P. Papazoglou, S. Schramm, J. Schaffner-Bielich, H. Stoecker, W. Greiner, Chiral Lagrangian for strange hadronic matter, Phys. Rev. C 57 (1998) 2576–2588, https://doi.org/10.1103/PhysRevC.57.2576, arXiv:nucl-th/9706024.

[30] P. Papazoglou, D. Zschiesche, S. Schramm, J. Schaffner-Bielich, H. Stoecker, W. Greiner, Nuclei in a chiral SU(3) model, Phys. Rev. C 59 (1999) 411–427, https://doi.org/10.1103/PhysRevC.59.411, arXiv:nucl-th/9806087.

[31] K. Tsubakihara, H. Maekawa, H. Matsumiya, A. Ohnishi, Lambda hypernuclei and neutron star matter in a chiral SU(3) relativistic mean field model with a logarithmic potential, Phys. Rev. C 81 (2010) 065206, https://doi.org/10.1103/PhysRevC.81.065206, arXiv:0909.5058.

[32] A. Mukherjee, J. Steinheimer, S. Schramm, Higher-order baryon number susceptibilities: interplay between the chiral and the nuclear liquid-gas transitions, Phys. Rev. C 96 (2) (2017) 025205, https://doi.org/10.1103/PhysRevC.96.025205, arXiv:1611.10144.

[33] A. Bazavov, et al., Fluctuations and correlations of net baryon number, electric charge, and strangeness: a comparison of lattice QCD results with the hadron resonance gas model, Phys. Rev. D 86 (2012) 034509, https://doi.org/10.1103/PhysRevD.86.034509, arXiv:1203.0784.

[34] S. Borsanyi, Z. Fodor, S.D. Katz, S. Krieg, C. Ratti, K. Szabo, Fluctuations of conserved charges at finite temperature from lattice QCD, J. High Energy Phys. 01 (2012) 138, https://doi.org/10.1007/JHEP01(2012)138, arXiv:1112.4416.

[35] D. Toublan, J.B. Kogut, The QCD phase diagram at nonzero baryon, isospin and strangeness chemical potentials: results from a hadron resonance gas model, Phys. Lett. B 605 (1–2) (2005) 129–136.

[36] A. Bhattacharyya, S. Das, S.K. Ghosh, R. Ray, S. Samanta, Fluctuations and correlations of conserved charges in an excluded volume hadron resonance gas model, Phys. Rev. C 90 (3) (2014) 034909, https://doi.org/10.1103/PhysRevC.90.034909, arXiv:1310.2793.

[37] R. Bellwied, S. Borsanyi, Z. Fodor, S.D. Katz, A. Pasztor, C. Ratti, K.K. Szabo, Fluctuations and correlations in high temperature QCD, Phys. Rev. D 92 (11) (2015) 114505, https://doi.org/10.1103/PhysRevD.92.114505, arXiv:1507.04627.

[38] A. Bhattacharyya, P. Deb, S.K. Ghosh, R. Ray, Investigation of the phase diagram and bulk thermodynamic properties using the Polyakov–Nambu–Jona-Lasinio model with eight-quark interactions, Phys. Rev. D 82 (1) (2010) 014021.

[39] A. Bhattacharyya, P. Deb, A. Lahiri, R. Ray, Susceptibilities with multiquark interactions in the Polyakov–Nambu–Jona-Lasinio model, Phys. Rev. D 82 (11) (2010) 114028.

[40] A. Bhattacharyya, P. Deb, A. Lahiri, R. Ray, Correlation between conserved charges in Polyakov–Nambu–Jona-Lasinio model with multiquark interactions, Phys. Rev. D 83 (1) (2011) 014011.

[41] A. Bhattacharyya, P. Deb, S.K. Ghosh, R. Ray, S. Sur, Thermodynamic properties of strongly interacting matter in a finite volume using the Polyakov–Nambu–Jona-Lasinio model, Phys. Rev. D 87 (5) (2013) 054009.

[42] A. Bhattacharyya, R. Ray, S. Sur, Fluctuation of strongly interacting matter in the Polyakov–Nambu–Jona-Lasinio model in a finite volume, Phys. Rev. D 91 (5) (2015) 051501.

[43] A. Bhattacharyya, S.K. Ghosh, S. Majumder, R. Ray, Study of beta equilibrated $2+1$ flavor quark matter in the Polyakov-Nambu-Jona-Lasinio model, Phys. Rev. D 86 (9) (2012) 096006.

[44] A. Bhattacharyya, R. Ray, S. Samanta, S. Sur, Thermodynamics and fluctuations of conserved charges in a hadron resonance gas model in a finite volume, Phys. Rev. C 91 (4) (2015) 041901.

[45] B. Klein, D. Toublan, J.J.M. Verbaarschot, The QCD phase diagram at nonzero temperature, baryon and isospin chemical potentials in random matrix theory, Phys. Rev. D 68 (2003) 014009, https://doi.org/10.1103/PhysRevD.68.014009, arXiv:hep-ph/0301143.

[46] D. Toublan, J.B. Kogut, Isospin chemical potential and the QCD phase diagram at nonzero temperature and baryon chemical potential, Phys. Lett. B 564 (2003) 212–216, https://doi.org/10.1016/S0370-2693(03)00701-9, arXiv:hep-ph/0301183.

[47] Y. Nishida, Phase structures of strong coupling lattice QCD with finite baryon and isospin density, Phys. Rev. D 69 (2004) 094501.

[48] A. Barducci, G. Pettini, L. Ravagli, R. Casalbuoni, Ladder QCD at finite isospin chemical potential, Phys. Lett. B 564 (2003) 217–224, https://doi.org/10.1016/S0370-2693(03)00705-6, arXiv:hep-ph/0304019.

[49] D. Toublan, B. Klein, J.J.M. Verbaarschot, The QCD phase diagram at non-zero baryon and isospin chemical potentials, Nucl. Phys. Proc. Suppl. 140 (2005) 562–564, https://doi.org/10.1016/j.nuclphysbps.2004.11.128, Nucl. Phys. Proc. Suppl. 562 (2004), arXiv:hep-lat/0409035.

[50] M.G. Alford, A. Kapustin, F. Wilczek, Imaginary chemical potential and finite fermion density on the lattice, Phys. Rev. D 59 (1999) 054502, https://doi.org/10.1103/PhysRevD.59.054502, arXiv:hep-lat/9807039.

[51] P. Kovács, Z. Szép, Influence of the isospin and hypercharge chemical potentials on the location of the critical end point in the μ_B–t phase diagram of the $su(3)_L \times su(3)_R$ chiral quark model, Phys. Rev. D 77 (2008) 065016, https://doi.org/10.1103/PhysRevD.77.065016, URL, https://link.aps.org/doi/10.1103/PhysRevD.77.065016.

[52] F. Becattini, M. Gazdzicki, J. Sollfrank, On chemical equilibrium in nuclear collisions, Eur. Phys. J. C 5 (1998) 143–153, https://doi.org/10.1007/s100529800831, arXiv:hep-ph/9710529, https://doi.org/10.1007/s100520050256.

[53] P. Braun-Munzinger, I. Heppe, J. Stachel, Chemical equilibration in Pb + Pb collisions at the SPS, Phys. Lett. B 465 (1999) 15–20, https://doi.org/10.1016/S0370-2693(99)01076-X, arXiv:nucl-th/9903010.

[54] A. Mukherjee, S. Schramm, J. Steinheimer, V. Dexheimer, The application of the Quark-Hadron Chiral Parity-Doublet model to neutron star matter, Astron. Astrophys. 608 (2017) A110, https://doi.org/10.1051/0004-6361/201731505, arXiv:1706.09191.

[55] J. Steinheimer, S. Schramm, The problem of repulsive quark interactions – lattice versus mean field models, Phys. Lett. B 696 (2011) 257–261, https://doi.org/10.1016/j.physletb.2010.12.046, arXiv:1005.1176.

[56] J. Steinheimer, S. Schramm, H. Stocker, An effective chiral Hadron-Quark equation of state, J. Phys. G 38 (2011) 035001, https://doi.org/10.1088/0954-3899/38/3/035001, arXiv:1009.5239.

[57] J. Steinheimer, V. Vovchenko, J. Aichelin, M. Bleicher, H. Stocker, Conserved charge fluctuations are not conserved during the hadronic phase, arXiv:1608.03737.

[58] J. Steinheimer, S. Schramm, H. Stocker, The hadronic SU(3) Parity Doublet Model for Dense Matter, its extension to quarks and the strange equation of state, Phys. Rev. C 84 (2011) 045208, https://doi.org/10.1103/PhysRevC.84.045208, arXiv:1108.2596.

[59] C. DeTar, T. Kunihiro, Linear sigma model with parity doubling, Phys. Rev. D 39 (1989) 2805–2808, https://doi.org/10.1103/PhysRevD.39.2805, URL, https://link.aps.org/doi/10.1103/PhysRevD.39.2805.

[60] T. Hatsuda, M. Prakash, Parity doubling of the nucleon and first order chiral transition in dense matter, Phys. Lett. B 224 (1989) 11–15, https://doi.org/10.1016/0370-2693(89)91040-X.

[61] S.A. Bass, P. Danielewicz, S. Pratt, Clocking hadronization in relativistic heavy-ion collisions with balance functions, Phys. Rev. Lett. 85 (13) (2000) 2689.

[62] F. Karsch, K. Redlich, Probing freeze-out conditions in heavy ion collisions with moments of charge fluctuations, Phys. Lett. B 695 (1–4) (2011) 136–142.
[63] A. Bazavov, H.-T. Ding, P. Hegde, O. Kaczmarek, F. Karsch, E. Laermann, S. Mukherjee, P. Petreczky, C. Schmidt, D. Smith, et al., Freeze-out conditions in heavy ion collisions from QCD thermodynamics, Phys. Rev. Lett. 109 (19) (2012) 192302.
[64] J. Rafelski, B. Muller, Strangeness production in the quark – gluon plasma, Phys. Rev. Lett. 48 (1982) 1066, https://doi.org/10.1103/PhysRevLett.48.1066, Erratum, Phys. Rev. Lett. 56 (1986) 2334, https://doi.org/10.1103/PhysRevLett.56.2334.
[65] C. Greiner, S. Leupold, Anti-hyperon production in relativistic heavy ion collision, J. Phys. G 27 (2001) L95–L102, https://doi.org/10.1088/0954-3899/27/9/102, arXiv:nucl-th/0009036.
[66] G. Torrieri, Resonances and fluctuations of strange particle in 200-GeV Au-Au collisions, J. Phys. G 32 (2006) S195–S204, https://doi.org/10.1088/0954-3899/32/12/S25, arXiv:nucl-th/0606009.
[67] C. Greiner, D.-H. Rischke, H. Stoecker, P. Koch, Creation of strange-quark-matter droplets as a unique signature for quark-gluon plasma formation in relativistic heavy-ion collisions, Phys. Rev. D 38 (9) (1988) 2797.
[68] J. Schaffner-Bielich, C. Greiner, H. Stöcker, A.P. Vischer, Properties of exotic matter for heavy-ion searches, J. Phys. G, Nucl. Part. Phys. 23 (12) (1997) 2107.
[69] J. Schaffner-Bielich, C. Greiner, A. Diener, H. Stöcker, Detectability of strange matter in heavy ion experiments, Phys. Rev. C 55 (6) (1997) 3038.
[70] J.D. Walecka, A theory of highly condensed matter, Ann. Phys. 83 (1974) 491–529, https://doi.org/10.1016/0003-4916(74)90208-5.
[71] M. Bender, P.-H. Heenen, P.-G. Reinhard, Self-consistent mean-field models for nuclear structure, Rev. Mod. Phys. 75 (2003) 121–180, https://doi.org/10.1103/RevModPhys.75.121.
[72] T.D. Cohen, R.J. Furnstahl, D.K. Griegel, Quark and gluon condensates in nuclear matter, Phys. Rev. C 45 (1992) 1881–1893, https://doi.org/10.1103/PhysRevC.45.1881.